

Supporting Information for:

Cd-containing quantum dots transform during simulated human digestion causing increased adverse subcellular effects to intestinal cells

Ke Xu^{1§}, Aude Bechu^{2§}, Connor Farrell², Niladri Basu³, Subhasis Ghoshal^{4*}, Saji George^{1*} and Audrey Moores^{2,5*}

¹ Department of Food Science and Agricultural Chemistry, McGill University, Montreal, Canada;

² Centre in Green Chemistry and Catalysis, Department of Chemistry, McGill University, Montreal, Canada; ³ Department of Natural Resources Sciences, McGill University, Montreal,

Canada; ⁴ Centre in Green Chemistry and Catalysis, Department of Civil Engineering, McGill University, Montreal, Canada; ⁵ Department of Mining and Materials Engineering, McGill

University, Montreal, Canada

Corresponding authors: audrey.moores@mcgill.ca, subhasis.ghoshal@mcgill.ca,

saji.george@mcgill.ca

Table of Contents

Materials and Methods	4
1. Simulated Digestion	4
2. Acid Digestion of centrifugal filtration samples:	5
3. Fluorescence dye mixtures composition	5
4. Calibration of spICP-MS:	5
5. Calculating number of QDs in aggregate compared to Cd particle size	6
6. Vetting sample preparation techniques for toxicity tests:	7
7. Tracking the capping polymer in simulated digestive system:	7
Supplemental results	9
1. Supplemental tables	9
Table S1: Composition of the digestion fluids (adapted from the Infogest protocol ¹).....	9
Table S2: Fluorophore cocktails used in the high content screening assays with detailed chemical information and principles of assays.	9
Table S3: Recoveries of ions, nanoparticle size, and nanoparticle concentration after the addition of 0.5 ppb of Cd ions.	10
2. Supplemental figures	11
Figure S1: Percent >3 kDa for ions (no QDs present) and polymer throughout digestion. ..	11
Figure S2: (A) Amount of QD aggregates in media > 210 QDs and (B) distribution of aggregates in the diluted media.	11
Figure S3: Relationship between Cd in Cd particle (spICP-MS result) and number of QD in aggregate (calculated).	12
Figure S4: (A) Representation of work-up of each aliquot at the digestion phase. (B) Recovery of QD after each digestion step. 100% indicates all of the expected Cd in the aliquot for salivary and gastric stages, while for the intestinal the 100% indicates the entire sample.	12

Figure S5: Recovery of polymer in the supernatant after ultracentrifugation of different digestion steps, compared to total polymer measured at each digestion step, by (A) $^1\text{H-NMR}$ (quantitative) and (B) IR (qualitative).	13
Figure S6: Calibration curve relating known concentration of polymer in a sample (x-axis) to the observed amount in solution (y axis $^1\text{H-NMR}$).	13
References.....	14

Materials and Methods

1. Simulated Digestion

Except for salivary amylase, enzymes were stored at -20°C as dry powders until the day they were suspended for use in a simulated digestion. Salivary amylase was suspended in solution at the concentration needed for digestion then stored at -20°C . The electrolyte composition of each digestion fluid is detailed in Table S1.

Potassium chloride ($>98\%$), monopotassium phosphate (99%), sodium bicarbonate ($\geq 99.7\%$), sodium chloride ($\geq 99\%$), magnesium chloride (99%), calcium chloride ($\geq 99\%$), sodium hydroxide (99.99%), and hydrochloric acid (37% v/v) were purchased from Sigma and used as received. These chemicals were used to make stock solutions, which were then combined into electrolyte-only simulated digestive fluids (Table S1, modeled after Brodkorb et al.¹)

Enzymes (and their activities) used in the digestions were salivary amylase (400 U/mg solid), pepsin (400 U/mg solid), pancreatin (4 U/mg solid) and bile salts (0.78 mmol of bile salts/g bile). These enzymes were used as received. Except for salivary amylase, enzymes were stored at -20°C as dry powders until the day they were suspended for use in a simulated digestion. Salivary amylase was suspended in solution at the concentration needed for digestion then stored at -20°C .

The composition of the digestive fluids were outlined in Figure 1 and Table S1.¹ Each digestion step was performed with prewarmed solutions (10 min) at 37°C , and each digestion step itself was performed at 37°C after mixing solutions at room temperature. Digestions were carried out in 20 mL glass vials.

2. Acid Digestion of centrifugal filtration samples:

The filtrate was added to a 50 mL tube, followed by 1 mL of H₂O₂ (Sigma, 50% reagent grade), and the resulting solution was digested at 95°C for 30 min. Then 1 mL of HNO₃ (99.999%, Trace Metal Grade) was added and the solution was digested at 95°C for 1 hour. After the two digestions the samples were diluted to 15 mL with water and transferred to tubes for ICP-OES analysis.

When the retentate sample was examined, H₂O₂ was first added to the filter and allowed to sit for 10 min. Then, it was transferred to the digestion tube for digestion at 95°C for 30 min. 1 mL of HNO₃ was also added to the filter for 10 min before being transferred to the digestion tube for digestion at 95°C for 30 min.

3. Fluorescence dye mixtures composition

The compositions of the four dye cocktails were summarized in Table S2. The first cocktail consisted of Hoechst 33342 (1 μM), DCF (10 μM), and LysoTracker (75nM) Hoechst 33342 (1 μM), the second cocktail was comprised of Fluo-4 (5 μM) and Propidium iodide (5 μM), the third cocktail contained Hoechst 33342 (1 μM) and MitoSox Red (5 μM), and the last cocktail included Hoechst 33342 (1 μM) and JC1 (1 μM). When performing the respective assays, 30 μL (cocktail 1 and 2) or 20 μL (cocktail 3 and 4) of dye cocktail was added to each well in the 384 well plate incubated for 30 min under standard culture conditions in the dark.

4. Calibration of spICP-MS:

The calibration of the single particle mode requires two key calibrations and method validation. The first key calibration step is transport efficiency. We used 30 nm Au NPs from NIST because preliminary tests of QDs in water indicated that their size range was ~25nm. We verified that

transportation efficiency of gold nanoparticles would not change significantly depending on the digestion stage (all were within the average $8.9 \pm 0.9\%$).

The next calibration necessary for measuring Cd in single particle mode is the dissolved ion calibration, which was achieved with an $R^2 = 0.9999$. However, Cd ions were not stable in deionized water, so spiking and recovering dissolved Cd in the presence of Cd-containing QDs was adjusted. We added 100 ppb EDTA to solutions of 10 ppb Cd ions in deionized water and stirred at 100 rpm for 2 h. Although this only kept $\sim 10\%$ of Cd ions in solution, subsequent dilutions into DI water were stable and we used these Cd ion solutions to spike solutions of QDs in different diluted digestion solutions (Table S3)

These results demonstrate that nanoparticle size and concentration were very stable in the presence of spiked Cd ions. The expected ionic content of the solution was 10% higher than expected, so this consistent increase was accounted for in subsequent calculations for the main text.

5. Calculating number of QDs in aggregate compared to Cd particle size

$$N_{QD} = \frac{\frac{4}{3}\pi(d_{Cd}/2)^3\rho_{Cd}}{f_{Cd}}/m_{QD}$$

Where the N_{QD} is the number of QDs in the aggregate, d_{Cd} is the diameter of the Cd particle (generated by spICP-MS), ρ_{Cd} is the density of Cd, f_{Cd} is the weight fraction of Cd in the QD, and m_{QD} is the mass of one QD. Please note that these calculations only account for the inorganic portion of QDs, and do not include the polymer coating. This calculation allowed for the correlation of the Cd particle LOD to the LOD of QD aggregates (Figure S3).

6. Vetting sample preparation techniques for toxicity tests:

With the transformations understood, we now moved to prepare samples for HIEC-6 cell exposures. Exposing intestinal epithelial cells to digestion fluids directly caused adverse effects in the cells, so sample preparation is necessary (Figure S5A). We deactivated the enzymes by boiling and centrifuged the aliquots. After centrifugation, only the pellet was recovered, resuspended, and dosed to the cells. We then measured the recovery of Cd in the pellet by ICP-OES to determine the exact dose used for cell toxicity tests (Figure S5B). We performed these steps to deactivate enzymes and decrease ionic strength.

There is a large amount of QDs that are missing from the salivary stage aliquot, possibly still attached to the sides of the sample vial. Most of the Cd (70%) from the gastric stage aliquot is present in the pellet. For the intestinal stage, the maximum possible amount in the pellet would be 50% (since we analyzed the entire sample, rather than the aliquot), and therefore the 27% of the Cd in the pellet represents most of the Cd present, but not all. These recovery tests indicated significant adhesion of Cd onto the sample vial (blue portion). There is between 20-40% of Cd remaining on these glass vials, which was less than the 45% of Cd remaining when we employed plastic vials in initial tests (data not shown). These results point to the difficulty in standardizing sample preparation for in vitro toxicity tests.

7. Tracking the capping polymer in simulated digestive system:

In addition to the tracking of Cd during simulated digestion sample work up, we tracked the presence of the polymer. Since the polymer contributed to synergistic toxicity impacts, we hypothesized that its presence in the pellet could also be a source of toxicity. We examined the presence of the polymer quantitatively by ¹H-NMR in the salivary and gastric phases (bile in the

intestine gave too high of a background signal to identify polymer peaks, Figure S5A). We qualitatively tracked the polymer's C-H signal in IR as well (Figure S5B).

These $^1\text{H-NMR}$ results indicate that $\sim 100\%$ of the polymer is suspended in solution after centrifugation of the salivary phase. The loss of the ligand in the salivary is also mirrored in the IR results of the pellet. This indicates that quantum dots lose their polymer coating in the salivary stage work up. Gastric results are conflicting between techniques. There is no polymer detected in the supernatant via $^1\text{H-NMR}$, which measures the phenol ring of the polymer. However, FTIR spectrum observed a decreased peak in the NH stretch region for SGF-QD from the previous stage (SSF-QD), suggesting possible loss of the ligand on the particles surface. Intestinal results are clouded by the presence of bile, a biomolecule whose concentration is at least 50-fold higher than the polymer, and includes phenolic and amine groups. Bile was present in both the supernatant and the pellet and FTIR spectrum showed the adsorption of bile molecules on the surface of the QDs. However, $^1\text{H-NMR}$ did not yield meaningful results because of the high background noises. More targeted analysis techniques will be necessary to elucidate the fate of the polymer in the simulated digestive system.

Supplemental results

1. Supplemental tables

Table S1: Composition of the digestion fluids (adapted from the Infogest protocol¹).

Name	Concentration in SSF (mM)	Concentration in SGF (mM)	Concentration in SIF (mM)
KCl	15.1	6.9	6.8
KH ₂ PO ₄	3.7	0.9	0.8
NaHCO ₃	13.6	25	85
NaCl	–	47.2	38.4
MgCl ₂ (H ₂ O) ₆	0.15	0.12	0.33
(NH ₄) ₂ CO ₃	0.06	0.5	–
HCl	1.1	15.6	8.4
CaCl ₂ (H ₂ O) ₂	1.5	0.15	0.6

Table S2: Fluorophore cocktails used in the high content screening assays with detailed chemical information and principles of assays.

	<i>Fluorophore</i>	<i>Target</i>	<i>Working concentration</i>	<i>Assay principle</i>
<i>Dye cocktail 1</i>	Hoechst 33342	Nucleus	1 μM	Nucleus stain that emits blue fluorescence upon bind to dsDNA.
	2',7'-dichlorodihydrofluorescein diacetate (H ₂ DCFDA)	Intracellular reactive oxygen species (H ₂ O ₂)	10 μM	Nonfluorescent dye that can be oxidized by reactive oxygen species into highly fluorescent DCF.
	LysoTracker	Acidic organelles	75 nM	Red fluorescent dye that stains acidic organelles (e.g. lysosomes)
<i>Dye cocktail 2</i>	Hoechst 33342	Nucleus	1 μM	Nucleus stain that emits blue fluorescence upon bind to dsDNA.

	Fluor 4	Intracellular [Ca ²⁺] flux	5 μM	Calcium indicator that increases fluorescence when binding to cytosolic Ca ²⁺ ions.
	Propidium Iodide	Plasma membrane damage	5 μM	Nucleus dye that enters cells with compromised membrane and fluoresces red
<i>Dye cocktail 3</i>	Hoechst 33342	Nucleus	1 μM	Membrane permeating nucleus stain that emits blue fluorescence upon bind to dsDNA.
	MitoSOX	Mitochondria puperoxide	5 μM	Red fluorescence dye that reacts to mitochondrial superoxide
<i>Dye cocktail 4</i>	Hoechst 33342	Nucleus	1 μM	Nucleus stain that emits blue fluorescence upon bind to dsDNA.
	JC-1	Mitochondria membrane depolarization	1 μM	Mitochondrial dye that fluoresces red when aggregated at polarized mitochondria membrane but shifts to green with a drop in the mitochondrial membrane potential

Table S3: Recoveries of ions, nanoparticle size, and nanoparticle concentration after the addition of 0.5 ppb of Cd ions.

Sample Matrix	Recovery of spiked dissolved ion as dissolved ion in reading	Recovery of same particle size of QDs after ion spike	Recovery of same particle concentration of QDs after ion spike
Media	N/A	96%	96%
Salivary	111%	98%	99%
Gastric	112%	83%	98%

2. Supplemental figures

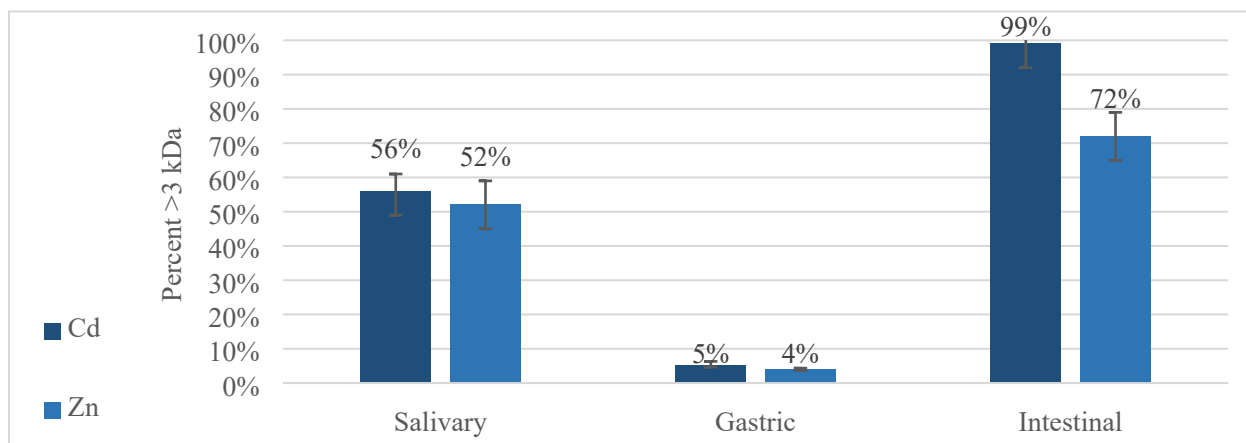


Figure S1: Percent >3 kDa for ions (no QDs present) and polymer throughout digestion.

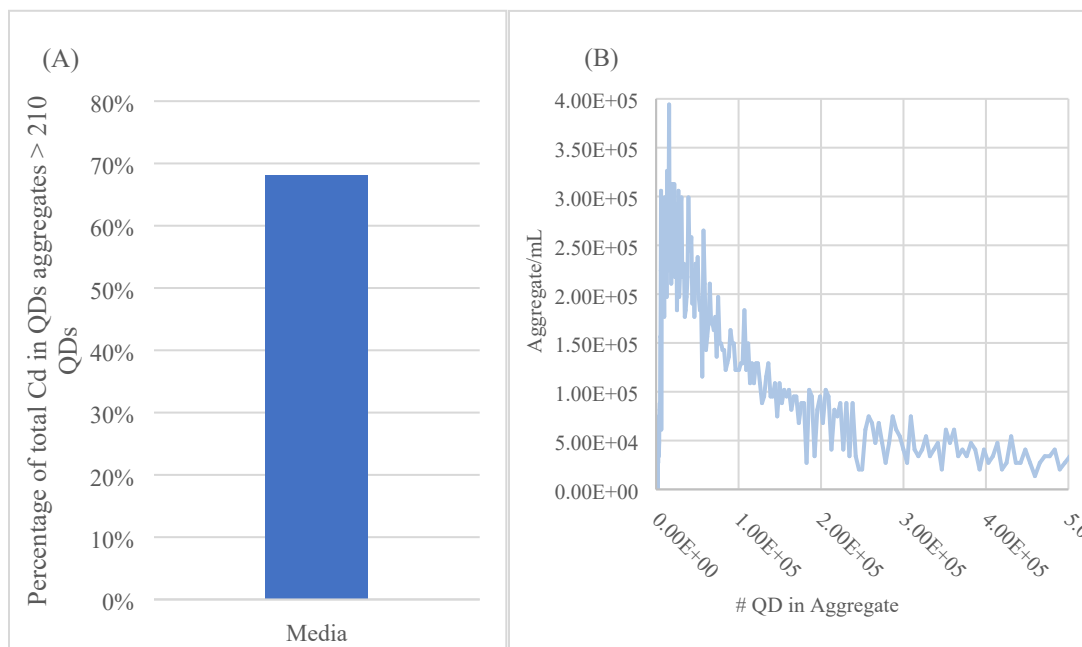


Figure S2: (A) Amount of QD aggregates in media > 210 QDs and (B) distribution of aggregates in the diluted media.

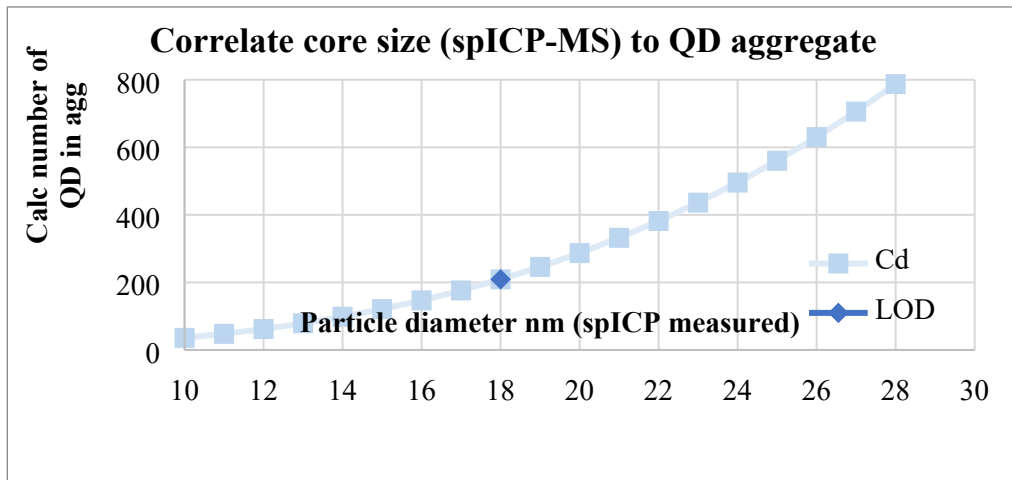


Figure S3: Relationship between Cd in Cd particle (spICP-MS result) and number of QD in aggregate (calculated).

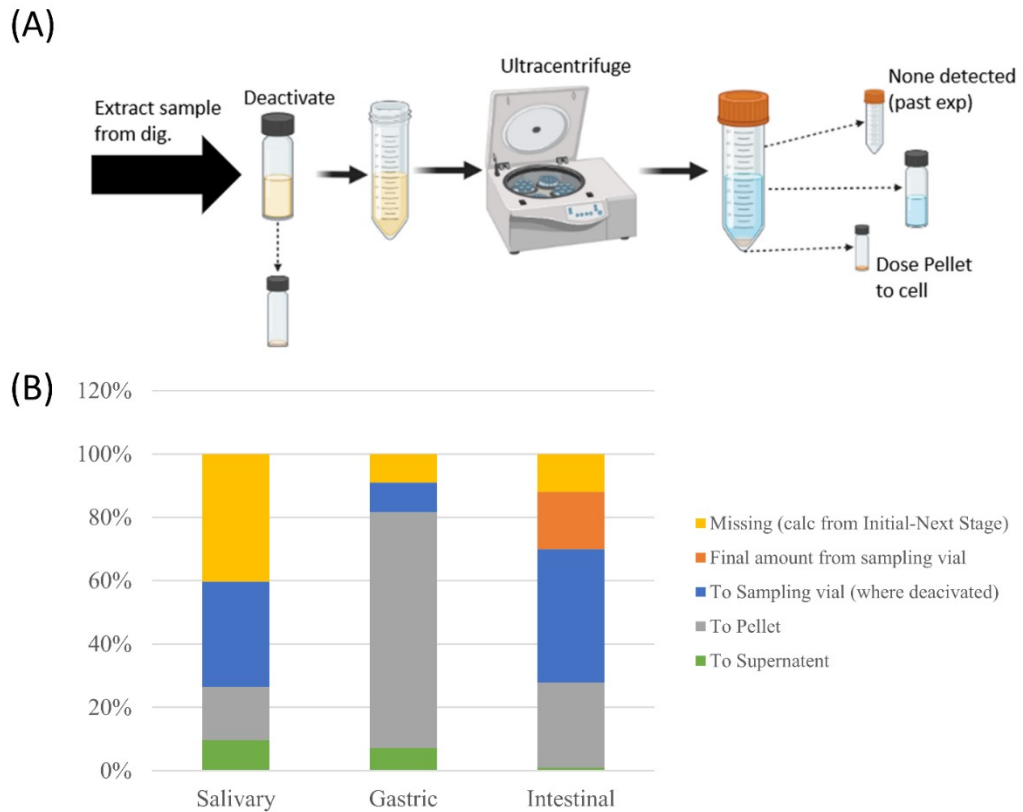


Figure S4: (A) Representation of work-up of each aliquot at the digestion phase. (B) Recovery of QD after each digestion step. 100% indicates all of the expected Cd in the aliquot for salivary and gastric stages, while for the intestinal the 100% indicates the entire sample.

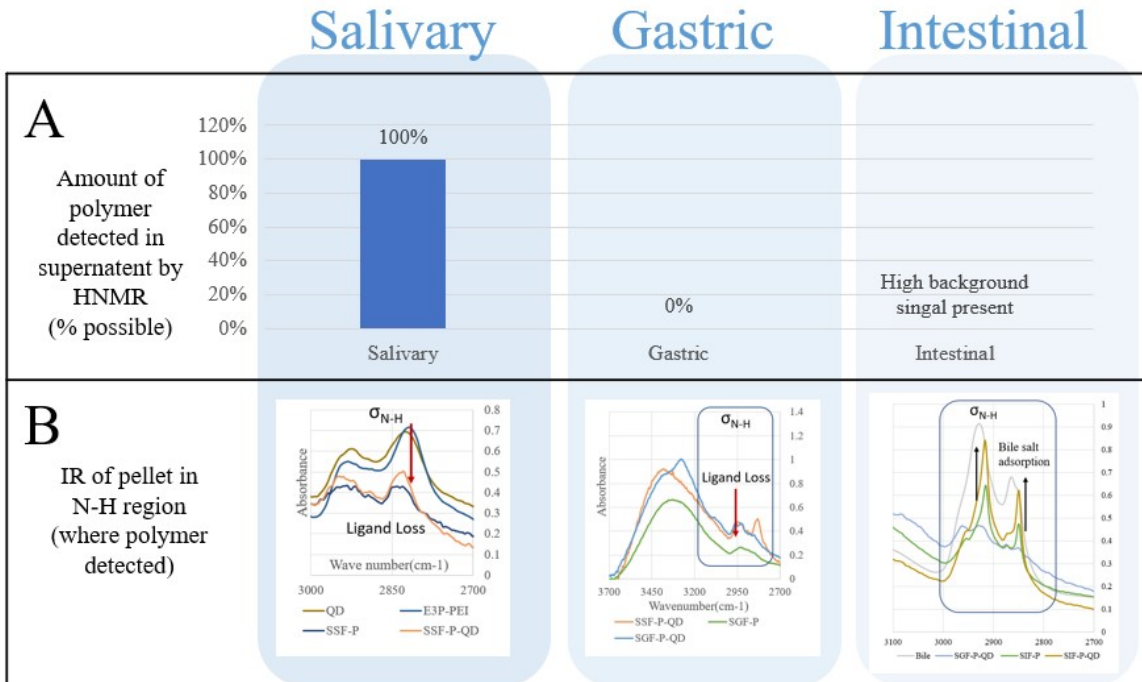


Figure S5: Recovery of polymer in the supernatant after ultracentrifugation of different digestion steps, compared to total polymer measured at each digestion step, by (A) ¹H-NMR (quantitative) and (B) IR (qualitative).

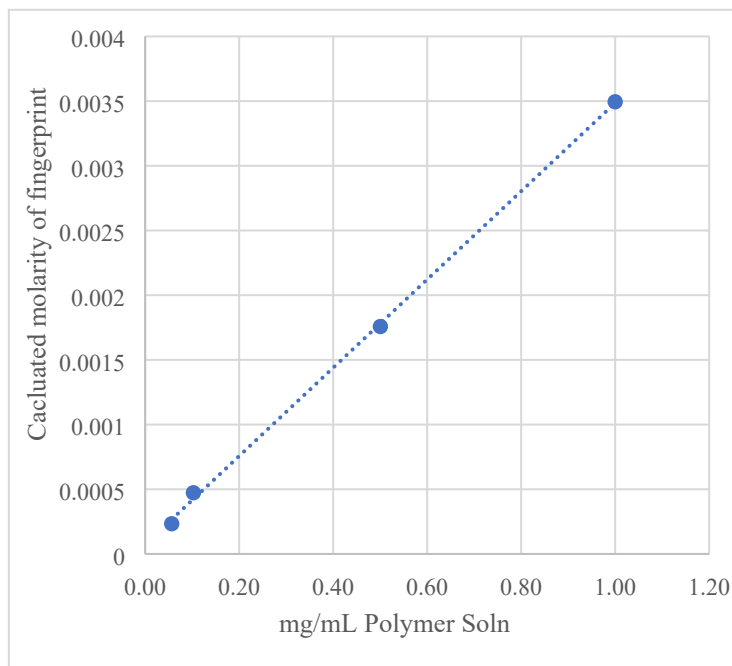


Figure S6: Calibration curve relating known concentration of polymer in a sample (x-axis) to the observed amount in solution (y axis $^1\text{H-NMR}$).

References

(1) Brodkorb, A.; Egger, L.; Alminger, M.; Alvito, P.; Assunção, R.; Ballance, S.; Bohn, T.; Bourlieu-Lacanal, C.; Boutrou, R.; Carrière, F. INFOGEST static in vitro simulation of gastrointestinal food digestion. *Nature protocols* **2019**, *14* (4), 991-1014.